

## Probing the magnetization inside a superconducting Nb film by nuclear resonant scattering

S. Couet,<sup>1,a)</sup> M. Trekels,<sup>1</sup> R. Ruffer,<sup>2</sup> J. Cuppens,<sup>3</sup> C. Petermann,<sup>1</sup> A. Vantomme,<sup>1</sup> M. J. Van Bael,<sup>3</sup> and K. Temst<sup>1</sup>

<sup>1</sup>*Instituut voor Kern- en Stralingsfysica and INPAC, K.U.Leuven, Celestijnenlaan 200D, B-3001 Leuven, Belgium*

<sup>2</sup>*European Synchrotron Radiation Facility (ESRF), BP 220, F-38043 Grenoble Cedex, France*

<sup>3</sup>*Laboratorium voor Vaste-Stoffysica en Magnetisme and INPAC, K.U.Leuven, Celestijnenlaan 200D, B-3001 Leuven, Belgium*

(Received 11 March 2011; accepted 27 July 2011; published online 31 August 2011)

We present an approach to probe the magnetization inside superconducting films using ultrathin <sup>57</sup>Fe probe layers excited by synchrotron radiation. We investigate the evolution of the <sup>57</sup>Fe hyperfine field orientation as a function of magnetic field above and below the superconducting transition temperature  $T_c$  for a Nb(50 nm)/<sup>57</sup>Fe(0.6 nm)/Nb(50 nm) trilayer. It is found that significant screening of the external field in the superconductor occurs only at low field, leading to a change in the hyperfine field angle below  $T_c$ . The presented approach allows to study the influence of magnetic fields and vortex induced electron correlations in complex layered structures incorporating superconductors. © 2011 American Institute of Physics. [doi:10.1063/1.3625941]

When applying an external magnetic field  $H_{ext}$  on type II superconductors, with  $H_{c1} < H_{ext} < H_{c2}$ , magnetic flux lines penetrate into the superconductor in the form of vortices, each carrying a flux quantum  $\phi_0$ . The core of a vortex has a diameter comparable to  $\xi$ , the superconducting coherence length. The magnetic field around the core is decreasing over a length  $\lambda$ , the penetration depth.<sup>1</sup> In thin films where the thickness becomes comparable to  $\lambda$ , the effective  $\lambda$  increases. This leads to a less pronounced magnetic field screening which will depend on the film thickness.<sup>2</sup> Although there is a vast amount of theoretical and experimental work (see Refs. 1–4 and references therein) on magnetic field screening and flux line lattices in superconductors, it has always remained a challenge to locally probe the magnetic field *inside* the superconductor. Imaging techniques with magnetic contrast, like scanning hall probe microscopy, can be used to visualize the flux line lattice at the surface of a thin film.<sup>5</sup> However, the strong diamagnetic response of the system prevents measuring the magnetization *inside* the film by conventional methods such as superconducting quantum interference device (SQUID) magnetometry. In the last decade, advanced techniques such as muon spin rotation ( $\mu$ SR) succeeded in retrieving information on the internal magnetic field present at the vortex cores.<sup>6</sup> With the availability of low energy (few keV) muons, it became possible to study thin films with  $\mu$ SR.<sup>7</sup> Another method used to probe inside the vortices in superconductor thin films is polarized neutron reflectometry, which can be used to retrieve the magnetization depth profile.<sup>8,9</sup> Since the magnetization of the superconductor is weak compared to that of a ferromagnetic material, experiments involving hybrid systems composed of magnetic and superconducting layers are practically out of reach of these methods.

In this letter, we present an alternative approach to probe the internal magnetization within superconductor films. The

method is based on nuclear resonant scattering (NRS) of synchrotron radiation using isotopic probe layers. This isotope-sensitive technique probes the local hyperfine field present at the nucleus of specific Mössbauer isotopes such as <sup>57</sup>Fe or <sup>119</sup>Sn.<sup>10–12</sup> In general, the magnetic field at the nucleus position is the sum of the hyperfine field generated by the electron shell and the external magnetic field. Hence, the magnetic field at the position of the Mössbauer isotope can be accessed. Since the NRS signal originates solely from the <sup>57</sup>Fe atoms, selective doping can be used to enhance sensitivity to specific parts of the system.<sup>13,14</sup> Here, we show that ultrathin <sup>57</sup>Fe layers can be used to measure the magnetization inside a superconducting film. We demonstrate this approach by measuring the magnetic response of a Nb/Fe/Nb trilayer, allowing to investigate the magnetic field screening in the superconducting layer, and to deduce the evolution of the sample's magnetization upon applying a magnetic field. This proof of principle experiment opens opportunities, particularly for the study of ferromagnet/superconductor hybrids, where proximity effects lead to strong interfacial interactions.

A trilayer of Nb(50 nm)/<sup>57</sup>Fe(0.6 nm)/Nb(50 nm) was grown by molecular beam epitaxy on a MgO(100) substrate held at 150 °C during deposition. Such a thin Fe layer allows superconducting coupling between the two Nb layers,<sup>15</sup> hence they can be treated as one 100 nm Nb film. Nb was deposited from an electron-gun source at a rate of 0.1 nm/s. Isotopically enriched (>95%) <sup>57</sup>Fe was evaporated from a Knudsen cell at a rate of 0.0035 nm/s. The sample was then covered with an 8 nm Si capping layer. A superconducting transition temperature  $T_c$  of 8.3 K was determined by SQUID. The NRS experiment was carried out at the ID18 beamline of the ESRF (Grenoble, France).<sup>16</sup> The sample was placed in a cryomagnetic system such that the applied magnetic field was perpendicular to the sample surface while the x-ray beam impinged at grazing incidence. Four

<sup>a)</sup>Electronic mail: sebastien.couet@fys.kuleuven.be.

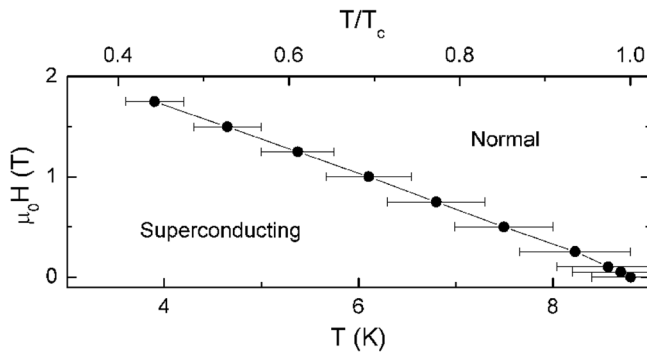


FIG. 1. Superconducting phase boundary of the Nb(50 nm)/Fe(0.6 nm)/Nb(50 nm) trilayer measured *in situ* with the magnetic field applied perpendicularly to the sample surface.

electrical contacts were used to monitor the electrical resistance throughout the experiment, allowing to track the superconducting phase transition. From the linear part of the phase boundary shown in Fig. 1, we can estimate the 0 K in-plane superconducting coherence length  $\xi(0)$  =  $\sqrt{\frac{\phi_0}{2\pi T_c dH_{c2}/dT}}$  =  $10 \pm 2$  nm, which is slightly smaller than typical values around 15 nm reported for Nb films of similar thicknesses.<sup>15</sup>

The experiment was carried out as follows. First a nuclear time spectrum (the time dependent de-excitation of the  $^{57}\text{Fe}$  nucleus after prompt excitation with synchrotron radiation) was recorded at 15 K and 0 T. Subsequently, the sample was field cooled below  $T_c$  and time spectra were recorded at 80% of  $T_c(H)$  and at 3.2 K. The temperature was then raised back to 15 K and the magnetic field was increased. This procedure was repeated until  $H_{ext} > H_{c2}$ . With this scheme, the 15 K time spectra series act as a reference representing the non-superconducting state, i.e., the Nb is in the normal state and does not interfere magnetically with the neighboring

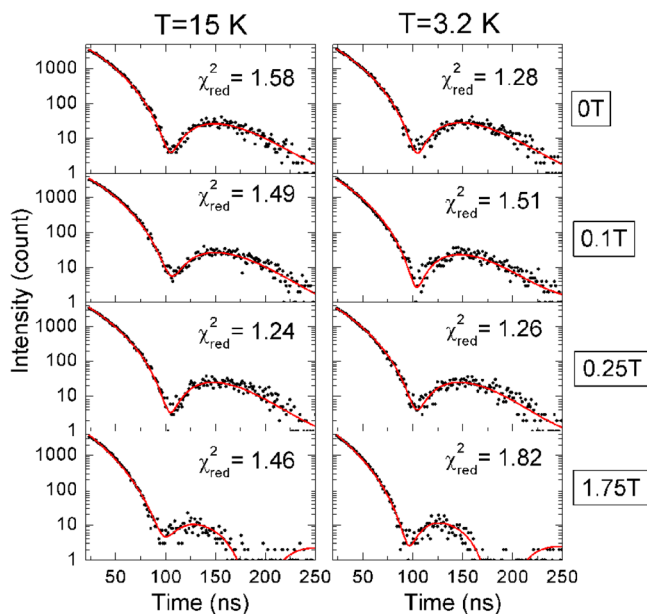


FIG. 2. (Color online) Selected nuclear time spectra recorded on the Nb/Fe/Nb trilayer above (left column) and below (right column)  $T_c$  for increasing magnetic field applied perpendicularly to the sample surface. The solid lines are fits.

TABLE I. List of fixed parameters for each component of the  $^{57}\text{Fe}$  layer used to fit the timespectra.

| Parameter for Fe             | Metallic | Interface |
|------------------------------|----------|-----------|
| Weight (%)                   | 52       | 48        |
| Isomer shift (mm/s)          | 0        | -0.31     |
| Hyperfine field $B_{hf}$ (T) | 33       | 33        |
| Flipping rate (GHz)          | 56       | 14        |

$^{57}\text{Fe}$  layer. Selected time spectra are shown in Fig. 2. Both data sets (above and below  $T_c$ ) show a similar trend, suggesting that the magnetic field almost completely penetrates the superconductor as soon as a small magnetic field is applied. Further quantitative information is gained by fitting the spectra.

We started by fitting the complete data set recorded at 15 K, using the CONUSS program.<sup>17</sup> Table I summarizes the basic parameters used to model the  $^{57}\text{Fe}$  layer, which is composed of an interfacial and a metallic Fe component. The isomer shift and weight of these components have been obtained by conversion electron Mössbauer spectroscopy measurements at room temperature. The other parameters have been determined by consistent fitting of the complete dataset such that the out-of-plane canting angle  $\theta_{meas}$  (see Fig. 3) is the only adjustable parameter. In order to reproduce the magnetic field dependence of the time spectra, we treated the Fe layer as a superparamagnetic medium, i.e., the local magnetization of the Fe atoms is continuously rotating at high frequency ( $>10$  GHz). Due to the strong shape anisotropy of this ultrathin film, we initially constrained the 33 T

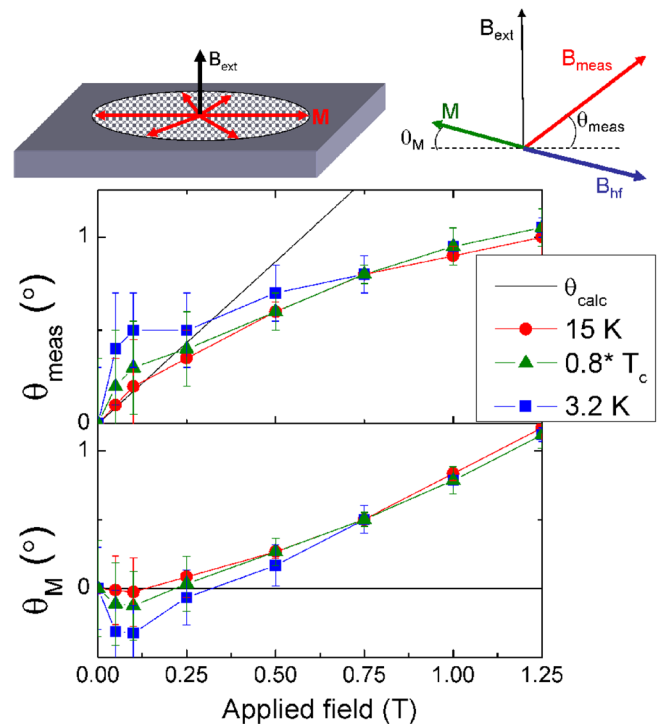


FIG. 3. (Color online) The top pictogram summarizes the model used for fitting the data: We use a superparamagnetic Fe layer constrained to flip in plane. We measure the angle  $\theta_{meas}$  which allows us to derive the magnetization angle  $\theta_M$ . The top and bottom panels show the evolution of  $\theta_{meas}$  and  $\theta_M$  with the external field, respectively.

hyperfine field of the Fe atoms to remain in the sample plane. It should be noted that this GHz flipping rate leads to a single line Mössbauer resonance in zero magnetic field (not shown). The fit yields the total field  $\mathbf{B}_{meas} = \mathbf{B}_{ext} + \mathbf{B}_{hf}$  at the Fe nucleus which makes an angle  $\theta_{meas}$  with the sample plane (see Fig. 3). It is assumed that the field at the position of the Fe atom ( $\mathbf{B}_{ext}$ ) equals the applied magnetic field and that the magnitude of  $\mathbf{B}_{hf}$  is fixed at 33 T. With this model, the field dependent data could be fitted assuming an average canting  $\theta_M$  of the magnetization  $\mathbf{M}$  towards the external field  $\mathbf{B}_{ext}$  direction, as shown in Fig. 3. It should be noted that the change of  $\theta_{meas}$  reflects in the slope of the decay while the isomer shift determines the position of the minima. The error bars on  $\theta_{meas}$  are calculated based on a 10% increase of the reduced  $\chi^2_{red}$  compared to its minimal value.<sup>18</sup> The larger error bars at low angles reflect a lower sensitivity in this range. Knowing the value of the external field  $\mathbf{B}_{ext}$  and assuming an in-plane hyperfine field  $\mathbf{B}_{hf}$ , we can calculate what should be the canting angle  $\theta_{calc}$ , i.e., the direction of the vector sum of  $\mathbf{B}_{ext} + \mathbf{B}_{hf}$ . As can be seen in Fig. 3, at 15 K the measured angle  $\theta_{meas}$  follows  $\theta_{calc}$  only below 0.25 T. The lower  $\theta_{meas}$  indicates that  $\mathbf{B}_{hf}$ , instead of remaining exactly in the film plane, points slightly away in the direction opposite to  $\mathbf{B}_{ext}$ . Since  $\mathbf{B}_{hf}$  is anti-parallel to the atom's magnetic moment, the sample magnetization  $\mathbf{M}$  is effectively canting towards the external field by an angle  $\theta_M$ .

When comparing the 15 K to the 3.2 K curve, we see clear differences at low field.  $\theta_{meas}$  is significantly increased at 3.2 K, while  $\theta_M$  is found to cant to the direction opposite to  $\mathbf{B}_{ext}$ . The measurements at 80% of  $T_c$  show a similar but reduced effect. At first thought, one could relate this to the screening of the applied field. This is indeed the regime where the density of vortices is low enough to observe a significant decrease of the magnetic field between them.<sup>18</sup> It should be noted that  $\theta_M$  is determined assuming that the field in the superconductor  $\mathbf{B}_{ext}$  is the same as the applied field, i.e. the superconductor does not screen the magnetic field. This assumption may not hold at fields below 0.2 T. When  $\mathbf{B}_{ext}$  is allowed to differ from the applied field, simple magnetic screening by the superconductor should lead to a reduction of  $\theta_{meas}$  compared to the non-superconducting state, rather than an increase, since the magnitude of the field  $\mathbf{B}_{ext}$  at the position of the probe would be smaller on average. This screening effect can therefore not explain the observed difference as it would lead to an even more negative value of the magnetization angle  $M$ . The reason for observing a negative polarization of the  $^{57}\text{Fe}$  is not clear at this stage. Another possibility is that the observed increase of  $\theta_{meas}$  is a more complex effect of the superconductor on the magnet, which may eventually lead to a specific polarization state due to the presence of Cooper pairs within the Fe layer.<sup>13</sup> Other effects beside the negative polarization of the Fe magnetization, that would lead to an observed increased  $\theta_{meas}$  are an increase of  $\mathbf{B}_{ext}$  or a decrease of  $\mathbf{B}_{hf}$ .

In conclusion, we have applied the technique of nuclear resonant scattering to probe the internal magnetization within a Nb thin film using an isotopic  $^{57}\text{Fe}$  probe layer in a superparamagnetic state. Detailed modeling of the system allows to measure the magnetization angle of the probe, and hence the magnetization at this position. We performed

measurements on a 100 nm Nb film incorporating a 0.6 nm  $^{57}\text{Fe}$  probe layer and showed that the average magnetization angle of the Fe film can be measured with high precision, leading to a high sensitivity to magnetization changes. This demonstrates the power of this approach to study the local magnetization in complex layered structures incorporating superconductors. In a broader scope, this approach enables to study complex ferromagnet/superconductor hybrids, where selective doping of  $^{57}\text{Fe}$  allows to retrieve depth dependent magnetization. In these systems, the interfaces are of particular interest since strong interactions are expected through the proximity effect. For the particular case presented here, experiments on films of different thicknesses will allow a detailed understanding of screening effects for thicknesses much larger than  $\lambda$ . The method can also be applied, with proper doping, to the recently discovered Fe-containing high  $T_c$  superconductor of the pnictide family,<sup>21</sup> since one can then probe the magnetization of the superconductor lattice, without incorporation of a foreign probe layer.

This work was supported by the Fund for Scientific Research-Flanders (FWO) as well as by the K.U.Leuven Concerted Action (GOA/09/006), the Belgian Interuniversity Attraction Poles research programs (IAP P6/42), by the K.U. Leuven BOF (CREA/07/005) program, the Centers of Excellence Programs (INPAC Grant No. EF/05/005). J.C. is grateful for the financial support by the Institute for the Promotion of Innovation in Flanders, IWT-Vlaanderen.

<sup>1</sup>E. H. Brandt, *Low Temp. Phys.* **36**, 5 (2010).

<sup>2</sup>B. Rosenstein and D. Li, *Rev. Mod. Phys.* **82**, 109 (2010).

<sup>3</sup>E. H. Brandt, *Rep. Prog. Phys.* **58**, 1465 (1995).

<sup>4</sup>A. I. Gubin, K. S. Ilin, S. A. Vitusevich, M. Siegel, and N. Klein, *Phys. Rev. B* **72**, 064503 (2005).

<sup>5</sup>J. R. Kirtley, *Rep. Prog. Phys.* **73**, 126501 (2010).

<sup>6</sup>J. E. Sonier, *Rep. Prog. Phys.* **70**, 1717 (2007).

<sup>7</sup>A. J. Drew, S. L. Lee, D. Charalambous, A. Potenza, C. H. Marrows, H. Luetkens, A. Suter, T. Prokscha, R. Khasanov, E. Morenzoni, D. Ucko, and E. M. Forgan, *Phys. Rev. Lett.* **95**, 197201 (2005).

<sup>8</sup>S.-W. Han, J. F. Anker, H. Kaiser, P. F. Miceli, E. Paroanu, and L. H. Greene, *Phys. Rev. B* **59**, 14692 (1999).

<sup>9</sup>A. J. Drew, M. W. Wisemayer, D. O. G. Heron, S. Lister, S. L. Lee, A. Potenza, C. H. Marrows, R. M. Dalgliesh, T. R. Charlton, and S. Langridge, *Phys. Rev. B* **80**, 134510 (2009).

<sup>10</sup>R. Röhlsberger, *Nuclear Condensed Matter Physics with Synchrotron Radiation, Springer Tracts in Modern Physics* (Springer, Berlin, 2004), Vol. 208.

<sup>11</sup>M. A. Andreeva, L. Häggström, B. Lindgren, B. Kalska, A.-M. Blixt, S. Kamali, O. Leupold, and R. Rüffer, *Hyperfine Interact.* **156/157**, 607 (2004).

<sup>12</sup>N. Planckaert, R. Callens, J. Demeter, B. Laenens, J. Meererschaut, W. Sturhahn, S. Kharlamova, K. Temst, and A. Vantomme, *Appl. Phys. Lett.* **94**, 224104 (2009).

<sup>13</sup>S. Couet, Th. Diederich, S. Stankov, K. Schlage, T. Slezak, R. Rüffer, J. Korecki, and R. Röhlsberger, *Appl. Phys. Lett.* **94**, 162501 (2009).

<sup>14</sup>B. Laenens, N. Planckaert, J. Demeter, M. Trekels, C. L'abbe, C. Strohm, R. Rüffer, K. Temst, A. Vantomme, and J. Meererschaut, *Phys. Rev. B* **82**, 104421 (2010).

<sup>15</sup>G. Verbanck, C. D. Potter, V. Metlushko, R. Schad, V. V. Moshchalkov, and Y. Bruynseraede, *Phys. Rev. B* **57**, 6029 (1998).

<sup>16</sup>R. Rüffer and A. I. Chumakov, *Hyperfine Interact.* **97/98**, 589 (1996).

<sup>17</sup>W. Sturhahn, *Hyperfine Interact.* **125**, 149 (2000).

<sup>18</sup>S. D. Kelly, K. M. Kemner, G. E. Fryxell, J. Liu, S. V. Mattigod, and K. F. Ferris, *J. Phys. Chem. B* **105**, 6337 (2001).

<sup>19</sup>M. M. Doria, E. H. Brandt, and F. M. Peeters, *Phys. Rev. B* **78**, 054407 (2008).

<sup>20</sup>K. S. Ilin, S. A. Vitusevich, B. B. Jin, A. I. Gubin, N. Klein, and M. Siegel, *Physica C* **408–410**, 700 (2004).

<sup>21</sup>P. M. Grant, *Nature* **453**, 1000 (2008).